

Article

Not peer-reviewed version

miR-27a-3p via FTO is Involved in Arsenite-Induced Apoptosis of HT22 Cells

[Qiyao Zhang](#), Teng Ma, Yujie Wang, Shiqing Xu, Siqi Zhao, [Suhua Wang](#), [Xiaohui Wang](#)^{*}, [Li Wang](#)^{*}

Posted Date: 29 April 2024

doi: 10.20944/preprints202404.1935.v1

Keywords: miR-27a-3p; Arsenic; Apoptosis; Hippocampal



Preprints.org is a free multidiscipline platform providing preprint service that is dedicated to making early versions of research outputs permanently available and citable. Preprints posted at Preprints.org appear in Web of Science, Crossref, Google Scholar, Scilit, Europe PMC.

Copyright: This is an open access article distributed under the Creative Commons Attribution License which permits unrestricted use, distribution, and reproduction in any medium, provided the original work is properly cited.

Disclaimer/Publisher's Note: The statements, opinions, and data contained in all publications are solely those of the individual author(s) and contributor(s) and not of MDPI and/or the editor(s). MDPI and/or the editor(s) disclaim responsibility for any injury to people or property resulting from any ideas, methods, instructions, or products referred to in the content.

Article

miR-27a-3p via FTO is Involved in Arsenite-Induced Apoptosis of HT22 Cells

Qiyao Zhang, Teng Ma, Yujie Wang, Shiqing Xu, Siqi Zhao, Suhua Wang, Xiaohui Wang * and Li Wang *

School of Public Health, Baotou Medical College, Baotou 014040, Inner Mongolia, China; 2020400068@stu.btmc.edu.cn (Q.Z.); 102018924@btmc.edu.cn (T.M.); 2021400065@stu.btmc.edu.cn (Y.W.); 2022200097@stu.btmc.edu.cn (S.X.); sqtjzy@163.com (S.Z.); bt_wangshuhua@163.com (S.W.)

* Correspondence: 102018909@btmc.edu.cn (X.W.); 101995002@btmc.edu.cn (L.W.)

Abstract Environmental arsenic exposure is closely related to nerve damage, and chronic arsenic exposure will cause neurotoxicity and damage the nervous system. Recent research suggests miR-27a-3p is required for the progression of certain neurodegenerative and neuropsychiatric disorders. Nonetheless, the precise impact of miR-27a-3p on neuron functioning in the hippocampus remains unclear. In this investigation, models were established using arsenite-treated cells and mice to investigate this aspect. After male C57BL/6J mice were exposed to arsenite (0, 0.5, 5 or 50ppm) in drinking water for 48 weeks, Nissl staining, terminal deoxynucleotidyl transferase-mediated dUTP-biotin nick end labeling (TUNEL) assay, and Hematoxylin-Eosin (H&E) staining revealed an arsenite-induced neuronal injury and apoptosis. For 6 μ mol/L arsenite-treated HT22 cells, arsenite decreases miR-27a-3p levels and activated the FTO/DRP1 pathway. For arsenite-treated HT22 cells, the increases of FTO and DRP1 and p-DRP1 (Ser616) levels induced by arsenite were reversed by miR-27a-3p mimic. Furthermore, the increases of neuronal apoptosis and pro-apoptotic protein (Bax and Cleaved-caspase 3) levels as well as decreased levels of anti-apoptotic proteins Bcl-2 induced by arsenite were reversed by miR-27a-3p mimic in HT22 cells. Moreover, the decreases of MMP induced by arsenite were reversed by miR-27a-3p mimic. Overall, in HT22 cells exposed to arsenite, miR-27a-3p mitigates neuronal apoptosis, suggesting its potential utility in addressing arsenite accumulation and associated with brain pathologies. Dysregulated expression patterns of miRNAs in the hippocampus have emerged as pivotal elements in neuronal apoptosis linked to neurological dysfunction, with miR-27a-3p specifically implicated in apoptotic pathways.

Keywords: miR-27a-3p; Arsenic; Apoptosis; Hippocampal

1. Introduction

Arsenic is a global health concern and environmental contaminant, with its toxicity impacting millions of individuals worldwide [1]. miR-27a-3p is capable of ameliorating brain diseases produced by NaAsO₂ accumulation and toxicity [2,3]. However, the specific underlying mechanisms remain unclear. Currently, drug and surgical treatments for neurological impairment have limited efficacy, underscoring the urgent need for novel therapeutic strategies.

MicroRNA (miRNA) is a class of noncoding RNA influencing the progression of various disorders, such as neurological disorders [4,5]. Expression of miRNA abnormalities in the hippocampus has been associated with neurodegenerative disorders characterized by apoptosis [6]. The miR-27 gene family encompasses two similar members, miR-27a and miR-27b, widely distributed in vertebrates [7]. Moreover, miR-27a-3p promotes apoptosis [8,9]. miR-27a-3p is not known to play a role in neurological impairment or apoptosis. HT22 cells undergoing OGD/R-induced apoptosis displayed significant downregulation of miR-27a-3p [10]. However, its biological role in neurological impairment or apoptosis remains elusive. Notably, downregulation of miR-27a-3p was identified during OGD/R-associated HT22 apoptosis, whereas miR-27a-3p overexpression mimics overturned OGD-associated apoptosis in HT22 cells. Moreover, dosing with a miR-27a-3p

agomir significantly limited TUNEL positivity following cerebral ischemia/reperfusion injury (CI/R) utilizing an in vivo rat model [11]. Several neurological diseases may benefit from miR-27a-3p as a therapeutic approach. However, contradictions have been identified; for instance, downregulating miR-27a-3p levels improved sevoflurane-associated neurotoxicity and neuroplasticity [12]. This discrepancy spurred further examination of the regulatory role of miR-27a-3p on neuronal function. We conducted a study to evaluate how miR-27a-3p affects neuronal function in HT22 cells. These cells are frequently used in vitro as a model for neuroinflammation and cellular signaling pathways analysis.

The hippocampus is a vital area of the brain that performs essential functions in memory formation, learning, controlling emotions, and perceiving pain. The link between mitochondrial dysfunction and hippocampal neuronal damage has been investigated recently [13,14]. Mitochondrial membrane potential (MMP) is an early and critical indicator of apoptosis. SH-SY5Y cells exposed to As_2O_3 alone exhibit a significant reduction in MMP, suggesting mitochondrial dysfunction [15]. FTO, widely expressed in nervous tissue, regulates mitochondria-mediated apoptosis [16]. FTO-mediated FTO/DRP1 signaling contributes to apoptosis [17]. Through the analysis of bioinformatics data, it has been discovered that miR-27a-3p operates as a suppressor of cancer progression in glioma. This is achieved by directly binding to FTO, which results in the inhibition of its expression [18]. In our research, we examined how miR-27a-3p affects cell death and mitochondrial dysfunction induced by $NaAsO_2$ in HT22 cells. However, the precise link between miR-27a-3p and FTO with regard to neurological impairment and apoptosis remains uncertain.

This study explored the function of miR-27a-3p during apoptosis to contribute to developing more effective treatment approaches for patients undergoing apoptosis. To offer novel insights for improved treatment options, we examined miR-27a-3p activity throughout apoptosis.

2. Materials and Methods

2.1. Mice and Experimental Groups

Male C57BL/6J mice aged five weeks were obtained from Calvin Biotechnology Co., Ltd. (Inner Mongolia, China). Experimental treatments received approval from the Experimental Animal Ethics Committee of Baotou Medical College. $NaAsO_2$ -treated mice were separated into classes, including (1) 0 ppm $NaAsO_2$ group, (2) 0.5 ppm $NaAsO_2$ group, (3) 5 ppm $NaAsO_2$ group, (4) 5 ppm $NaAsO_2$ group. $NaAsO_2$ was administered via drinking water with an exposure duration of 48 weeks.

2.2. H&E Staining

Brains were extracted for fixation and dehydration using gradient alcohol before being embedded in paraffin for sectioning at 3 μ m thick and incubated at 65 °C for 4.5 hours before dewaxing, hydrating, flushing, and staining with H&E (Baso, Zhuhai, China). Sections were observed using a fluorescent microscope (BX43, OLYMPUS, Japan).

2.3. Nissl Staining

Brain tissues were embedded in liquid paraffin, and sections were obtained at 3-5 μ m thickness. Xylene was employed for dewaxing, and alcohol was used for rehydration. The brain tissues were stained with Nissl stain and randomly examined by pathologists.

2.4. TUNEL

Brain tissues underwent paraffin embedding and sectioning. Proteinase K was used to treat tissues at 37° C for 20 minutes and washed three times with PBS. TUNEL staining followed the instructions of the TUNEL Apoptosis Detection Kit (Beyotime Biotechnology, Shanghai, China). The fluorescence signals were characterized utilizing an OLYMPUS fluorescence microscope (BX43, Japan).

2.5. Real-Time Fluorescence Quantitative PCR (RT-qPCR)

Adhering to the manual, total RNA was isolated from HT22 cells with TRIzol (TransGen Biotech, Beijing, China). Moreover, total RNA quality and quantity were investigated utilizing a NanoDrop (ThermoFisher Scientific, USA). After RNA harvest, it was reverse transcribed using a Veriti Thermal Cycler (Applied Biosystems, USA). Real-time quantitative PCR (qPCR) was conducted using GoTaq® qPCR Master MixA6001 (Promega, USA), utilizing U6 as internal controls. Primers utilized in this study were: miR-27a-3p: TCCACAGTGGCTAAGTTCCGC, GCGCTAGCACCATTTGAAATCAGTGT. qPCR reactions were all conducted using three replicates, and gene expression fold changes were computed using the $2^{-\Delta\Delta C_t}$ method.

2.6. Culture of Mouse Hippocampal HT22 Cells and Experimental Groups

Cells were obtained from Preicella (Wuhan, China). Cultures were kept at a concentration of 5×10^5 cells/mL in DMEM alongside 10% fetal bovine serum (FBS), penicillin G (100 U/mL), and streptomycin (100 mg/L) at 37 °C under humid conditions with 5% CO₂. The cells were split when they reached 70% to 90% confluence. The growth media was replenished every two days, and the arsenic exposure group was exposed to a concentration of 6 μmol/L for 24h.

2.7. Cell Viability Assessment

The cell sustainability was characterized using a Cell Counting Kit-8 (Biosharp, China). HT22 cells were cultured in 96-well plates (with 5000 cells in each well) alongside dissolved NaAsO₂ for 24h. A sample of 10 μL of CCK-8 reagent was included, and a 2-hour incubation at 37 °C was executed. Each well underwent examination using 450 nm light in a microplate reader (BioTek Instruments). The cell survival rate (%) = (OD experimental - OD blank) / (ODcontrol - ODblank) × 100%.

2.8. Transient Cell Transfection

HT22 cells underwent transfection using miR-27a-3p mimic (micrON mmu-miR-27a-3p mimic, Cat# miR10000537-1-5, Ribobio), or a corresponding scrambled control (micrON miRNA mimic Ncontrol #22, Cat# siN0000001-1-5, Ribobio) with Lipofectamine 2000 (Invitrogen) adhering to the manufacturer's directions. Upregulation of miR-27a-3p was examined via RT-PCR six hours following the transfection took place.

Transfections were conducted in 6-well plates using 7.5 μL Lipofectamine 2000 in 100 μL OptiMEM (1 X) Medium per well. The mimics were diluted in 100 μL OptiMEM (1 X) Medium per well. Following dilution, the miR-27a-3p mimic was combined with diluted Lipofectamine 2000 Reagent (1 : 1) and then maintained for 5 minutes at room temperature. After transfection, the complex was mixed with HT22 cells in 1787.5 μL Opti-MEM (1 X) Medium and incubated for six hours. Following the six-hour incubation, the transfection media was removed, and new media was included. Cells were maintained for 24 hours before undergoing examination.

2.9. Apoptosis Assay

As indicated by the manufacturer, Annexin V FITC/PI staining flow cytometry was utilized to examine apoptosis of HT22 cells. The cells were harvested in centrifuge tubes, and resuspended in cool PBS (1 X) (Gibco, USA) twice at 800 rpm for 4 minutes, removing the supernatant each time. Cells were then resuspended with 200 μL of Binding Buffer, 2 μL Annexin-V-FITC, and 2 μL PI and were maintained in the absence of light at room temperature for 15 minutes, followed by apoptosis characterization by CytoFLEX flow cytometry (Beckman Coulter, USA).

2.10. Western Blot

Lysate proteins were assayed via a BCA (Applygen, China). Equal concentrations of protein were electrophoresed using SDS acrylamide gels. Protein bands were transferred onto PVDF

membranes. The membrane was maintained at room temperature for two hours and mixed with primary antibodies at 4 °C overnight. These antibodies encompassed anti-FTO, anti-DRP1, anti-p-DRP1 (Ser616), anti-Bax, anti-Bcl-2, or anti-Cleaved-caspase 3. The rinsed membranes were maintained for 1 hour with HRP-labeled goat anti-mouse secondary antibody (Signalway Antibod, USA). Visualization of bands was undertaken and positive protein signals on membranes were captured by an enhanced chemiluminescence light method (The company). β -actin was employed as a standard. Data analysis was performed using Image J (NIH, USA).

2.11. Mitochondrial Membrane Potential Assay

We investigated MMP activity in HT22 cells using the JC-1 probe (Beyotime Biotechnology, Shanghai, China). Cells were mixed with JC-1 (2 μ M) at 37 °C for 30 minutes. To characterize HT22 MMP, fluorescence microscopy measured alterations in JC-1-associated fluorescence ranging from red (J-aggregates) to green (monomeric). The fluorescence intensity was examined using Image J (NIH, USA) to investigate the differences in MMP.

2.12. Statistical Analysis

Data are presented as the mean and standard deviations (SDs). GraphPad Prism 9.0 was employed to produce graphics and assess statistical data. Variations between NaAsO₂ exposed and control groups were differentiated through one-way ANOVA. $p < 0.05$ represents statistical significance.

3. Results

3.1. Chronic Exposure of Mice to Arsenite Induce Apoptosis of Hippocampus

To investigate the impact of arsenite on neuron mortality and deterioration, we performed H&E, TUNEL, and Nissl staining were conducted on the arsenite-treated brain tissues from C57BL/6J mice. In histopathological analysis, diffuse nuclear pycnosis, hyperstaining, and neuronal vacuolation were increased following arsenite exposure relative to the control group, as indicated by H&E staining. In contrast to the control group, the arsenite exposure group showed higher levels of TUNEL-positive and apoptotic neuronal cells (Figure 1A-C).

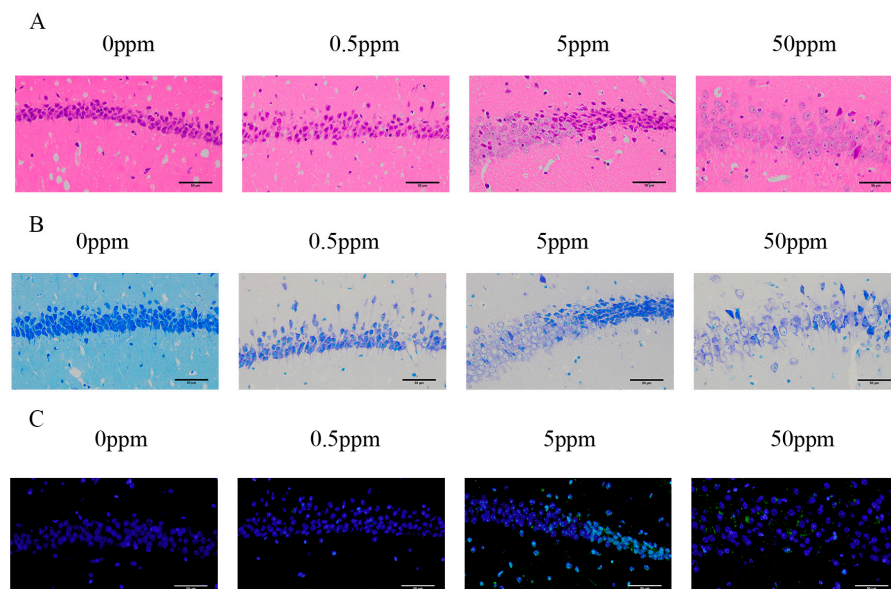


Figure 1. Chronic exposure of mice to arsenite induce apoptosis of hippocampus. Mice were exposed to arsenite (0, 0.5, 5 or 50 ppm) in drinking water for 48 weeks. (A) H&E staining implemented for

monitoring histomorphologic features of brain tissue. (B) The levels of TUNEL-positive cells with TUNEL levels. (C) The number of apoptotic neurons observed with Nissl staining.

3.2. Arsenite Induce Decrease of miR-27a-3p Levels, Inhibition of miR-27a-3p Increase the Cell Viability in Arsenite-Treated HT22 Cells

To mirror damage in vitro, the arsenite -treated cell model was characterized. arsenite inhibits miR-27a-3p production in HT22 cells, which is inverted by miR-27a-3p mimics (Figure 2A). Moreover, arsenite significantly lowered the persistence of HT22 cells, whereas miR-27a-3p mimics significantly reversed this effect (Figure 2B). Additionally, negative control microRNA (miR-NC) marginally impacted the persistence of HT22 cells (Figure 2B). These data indicated that arsenite -associated hindrance of HT22 cell proliferation is upended by miR-27a-3p mimics.

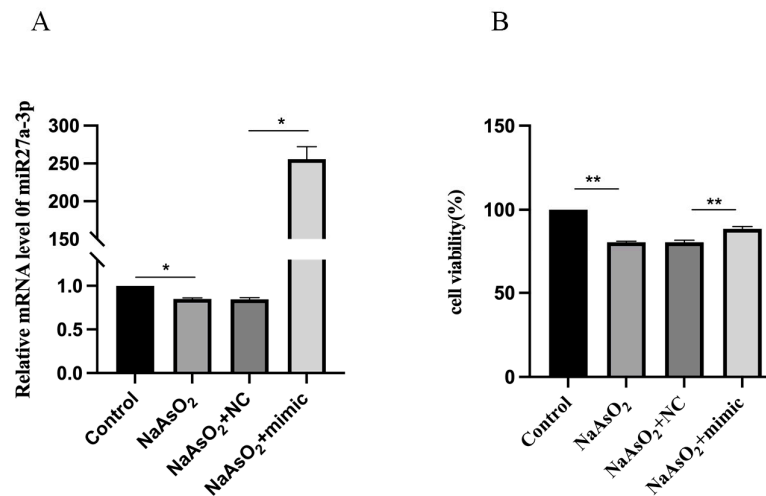


Figure 2. Arsenite induce decrease of miR-27a-3p levels, inhibition of miR-27a-3p increase the cell viability in arsenite-treated HT22 cells. HT22 cells were treated with 0 or 50nM miR-27a-3p mimic/NC for 30 min, then exposed to 0 or 6 μ M arsenite for 24 h. (A) Production of miR-27a-3p in HT22 cells(mean \pm SD, n = 3). (B) HT22 cells examined using CCK-8 (mean \pm SD, n = 3). * p < 0.05, ** p < 0.01 vs. Control or NaAsO₂+NC.

3.3. miR-27a-3p via FTO/DRP1 Axis Overcomes the Damage in Arsenite-Treated HT22 Cells

The gene specifically tuned by miR-27a-3p was examined using the NCBI online tools. FTO is a possible position of action for miR-27a-3p (Figure 3A). Western blot was performed to investigate the mechanisms arsenite uses to regulate apoptosis in vitro. The expression of FTO, DRP1, and p-DRP1 (Ser616) in HT22 cells was elevated by arsenite treatment. However, this impact was inhibited when miR-27a-3p mimics were present (Figure 3B–E). These findings suggest that apoptosis induction in HT22 cells by arsenite is mediated by activating the FTO/DRP1 pathway, which can be overcome by miR-27a-3p.

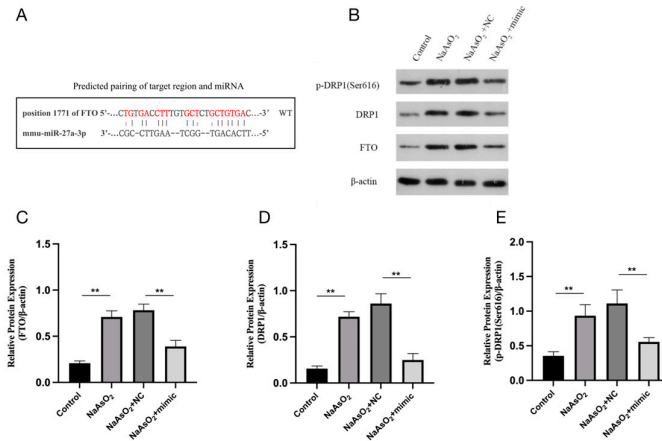


Figure 3. miR-27a-3p via FTO/DRP1 axis overcomes the damage in arsenite-treated HT22 cells. HT22 cells were treated with 0 or 50nM miR-27a-3p mimic/NC for 30 min, then exposed to 0 or 6 μM arsenite for 24 h. (A) The genetic arrangement of FTO at position 1771 indicates a putative binding location for miR-27a-3p within its 3' UTR. (B) Western blot indicating expression of FTO, DRP1, and p-DRP1 (Ser616) in HT22 cells. (C-E) Comparative production of FTO (C), DRP1 (D), and p-DRP1 (Ser616) (E), compared to β-actin (mean ± SD, n = 3). ***p* < 0.01 vs. Control or NaAsO₂+NC.

3.4. miR-27a-3p via FTO/DRP1 Axis Inhibit the Apoptosis in Arsenite-Treated HT22 Cells

We employed flow cytometry to identify apoptosis and found that HT22 cells experienced significantly increased apoptosis upon exposure to arsenite (Figure 4A, B). Similar to the observed increase in apoptosis, arsenite produced a notable increase in active Bax and Cleaved-caspase 3, both pro-apoptotic enzymes (Figure 4C, E-F). In contrast, arsenite produced a considerable reduction in anti-apoptotic protein (Bcl-2) levels in HT22 cells (Figure 4C-D). However, when miR-27a-3p mimics were introduced, these impacts were reversed (Figure 4A-F).

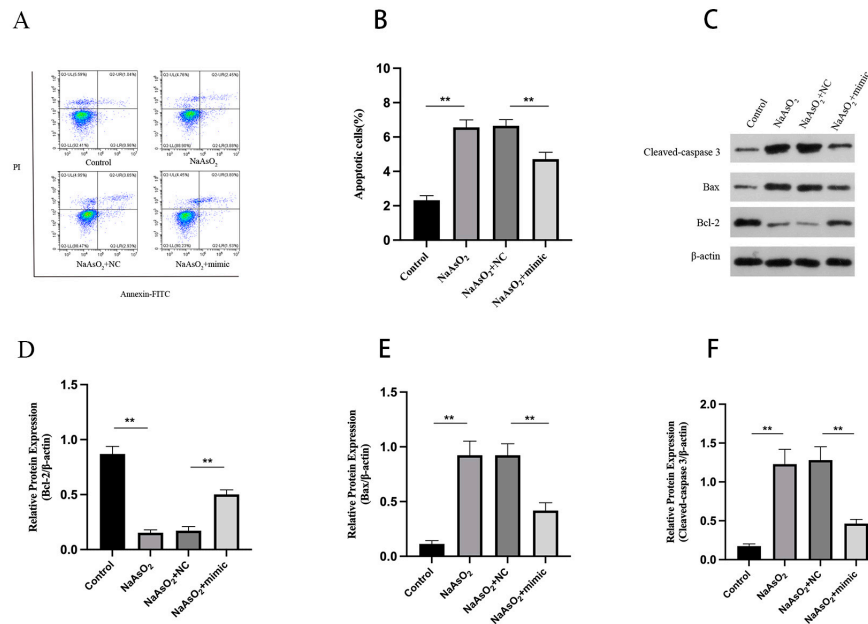


Figure 4. miR-27a-3p via FTO/DRP1 axis inhibit the apoptosis in arsenite-treated HT22 cells. (A) Flow cytometry examination of apoptosis. (B) Apoptotic rate in HT22 cells (mean ± SD, n = 3). (C) Western blot of Bcl-2, Bax, and Cleaved-caspase 3 in HT22 cells. (D-F) Comparative expression levels of Bcl-

2. Bax, and Cleaved-caspase 3 standardized to β -actin (mean \pm SD, n = 3). ** p < 0.01 vs. Control or NaAsO₂+NC.

3.5. miR-27a-3p via FTO/DRP1 Axis Inhibit the Level of MMP in Arsenite-Treated HT22 Cells

Utilizing a fluorescence microscope to characterize MMP levels in HT22 cells, we identified that arsenite significantly lowered MMP levels (Figure 5A, B). Again, the influence was overcome upon exposure to miR-27a-3p mimics (Figure 5A, B). Therefore, introducing miR-27a-3p effectively mitigates arsenite-associated damage to mitochondria in HT22 cells.

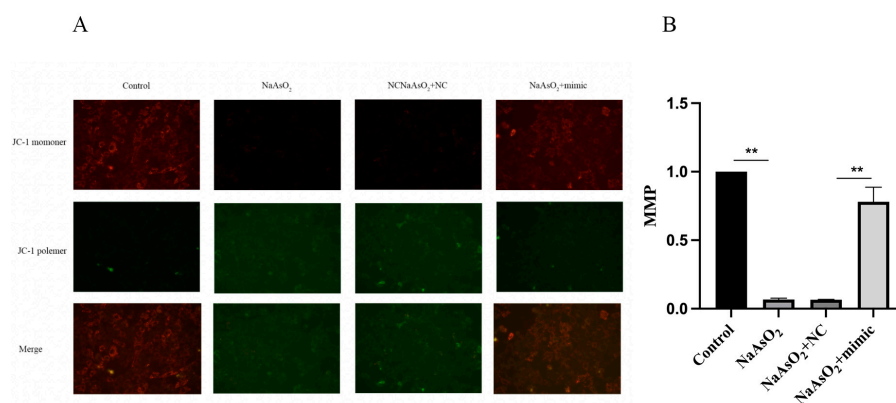


Figure 5. miR-27a-3p via FTO/DRP1 axis inhibit the level of MMP in arsenite-treated HT22 cells. HT22 cells were treated with 0 or 50nM miR-27a-3p mimic/NC for 30 min, then exposed to 0 or 6 μ M arsenite for 24 h. (A) Fluorescence examination of MMP levels in HT22 cells. (B) the levels of MMP (mean \pm SD, n = 3). ** p < 0.01 vs. Control or NaAsO₂+NC.

4. Discussion

Globally, arsenic exposure causes significant health problems and is a global public health concern [19]. The association between environmental arsenic exposure and nerve damage is becoming more evident with studies demonstrating that hippocampal neurons can undergo apoptosis as a result of prolonged arsenic exposure [20]. Arsenic exposure can lead to neurotoxicity by triggering apoptosis, but the exact mechanism is unknown. As a sensitive part of the brain to dysfunctional transition metal homeostasis, learning and memory formation, emotion regulation, and pain perception are significantly influenced by the hippocampus. Neurodegenerative diseases are closely associated with damaged hippocampal structure and function [21]. The in vivo findings of this study demonstrated that the administration of arsenite-induced histopathological alterations in hippocampal tissue and triggered apoptosis in hippocampal cells among C57BL/6J mice. MiRNAs function in apoptosis progression [22,23]. The study conducted by Chi B et al. demonstrated that elevated levels of miRNA-26a were associated with enhanced neuronal apoptosis in the brain [24]. The overexpression of miRNA-23a-3p rescued cardiomyocytes from apoptosis induced by high glucose [25]. HT22 cells exposed to arsenite showed significant decreases in miR-27a-3p levels determined by qRT-PCR. Our in vitro assessments suggested that apoptosis was enhanced in the arsenite-exposed mice. Our findings mirror earlier studies [26,27]. In our investigation, we found that the increase of apoptosis in arsenite-induced HT22 cells and substantially hindered by the administration of miR-27a-3p mimics. According to these findings, miR-27a-3p may contribute to neuronal injury and apoptosis induced by arsenite. Our examination explored the possible impact of miR-27a-3p on arsenite-induced cell death and highlighted its suppressive effect. A recent study uncovered that reducing miR-27a-3p levels enhanced cell development, LDH release, inflammation, and apoptosis caused by arsenite via NRIP1 targeting [28]. This suggests that the diverse functions of miR-27a-3p may contribute to its overall impact.

Traditionally, miRNAs exercise their influence by inhibiting the production of specific genes [29]. By reviewing literature and using bioinformatics databases NCBI, this study predicted and potential target genes of miR-27a-3p screened, and HT22 cells were predicted to undergo apoptosis as a result of arsenite-induced miR-27a-3p/FTO/DRP1 signaling. By activating its s616 phosphorylation level, DRP1 (Ser616) regulates mitochondrial fission and mitochondria-mediated endogenous apoptosis by up-regulating mitochondrial fission. FTO is produced in neurons across the brain, transiting between the nucleus and cytoplasm [30]. It functions in diverse biological processes and cell death, likely involved in apoptosis [31]. Through activation of the AKT/Nrf2 pathway, overexpression of FTO alleviates Cd-induced cell death and oxidative damage in granulosa cells [32]. Another study indicated that FTO inhibitors protect dopamine neurons from cell death produced by growth factor limitation [33]. These studies indicate that FTO expression is unstable in apoptosis. Our findings demonstrate that miR-27a-3p promotes FTO/DRP1 signaling, while the miR-27a-3p mimics exhibited an apparent reversal effect. These findings support the reliability of our results. FTO concentrations were suppressed by miR-27a-3p mimics, indicating that it inhibits arsenite-induced apoptosis progression through its excitatory effect on FTO/DRP1 signaling. In contrast, DRP1 promotes mitochondrial fission in healthy cells to maintain homeostasis, mediating mitochondrial fragmentation in apoptotic cells [34]. The levels of DRP1 and mitochondrial impairment were significantly elevated in both human OA cartilage and mouse joints undergoing DMM surgery, exhibiting elevated chondrocyte apoptosis [35]. In this work, the FTO/DRP1 signaling pathway was upregulated during arsenite-induced apoptosis in vitro model, and this was inverted by miR-27a-3p.

It has been widely reported that mitochondrial initiation is the main pathway causing apoptosis. This process decreases mitochondrial membrane potential and ultimately causes cell death [36]. As protein markers involved in apoptosis, Bax, Bcl-2, and Cleaved caspase 3 play a significant role in triggering apoptosis. As a result, the ratio of Bax to Bcl-2 and cleaved caspase 3 are often used to indicate apoptosis potential in cells [37]. According to the results of this experiment, HT22 cells treated with NaAsO₂+mimic showed reduced apoptosis rates and lowered levels of proteins that promote cell death Bax and Cleaved caspase 3. This indicated that miR-27a-3p expression level upregulation in HT22 cells effectively inhibits cell apoptosis induced by 6 mol/L NaAsO₂. To investigate if arsenite triggers apoptosis in HT22 cells is associated with miR-27a-3p-mediated mitochondrial damage, JC-1 probe and fluorescence microscopy were used to detect mitochondrial membrane potential. Behind transfection with miR-27a-3p mimic, the mitochondrial membrane potential was also reversed, indicating that miR-27a-3p mimic inhibited arsenite-induced mitochondrial damage. Overall, it was demonstrated that miR-27a-3p was involved in reversing mitochondrial damage and apoptosis induced by arsenite in HT22 cells, suggesting that miR-27a-3p may be able to regulate endogenous mitochondrial pathways that mediate apoptosis in HT22 cells.

5. Conclusions

In short, miR-27a-3p/FTO/DRP1 signaling pathway is responsible for the reduction in mitochondrial membrane potential caused by arsenic, ultimately leading to apoptosis in HT22 cells through the endogenous mitochondrial pathway. The introduction of a miR-27a-3p mimic was able to reverse the neuronal apoptosis triggered by arsenic (Figure 6). which provides clues for discovering biomarkers for the development of Neuro-related diseases and for prevention and treatment of arsenic poisoning.

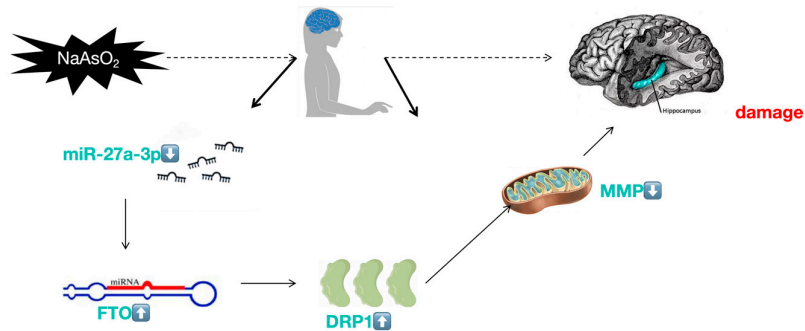


Figure 6. miR-27a-3p via FTO is involved in arsenite-induced apoptosis of HT22 cells.

Author Contributions: Q.Z.: design, data analysis, and draft of the manuscript. T.M. and S.W.: investigation and formal analysis. Y.W., S.Z. and S.X.: software and resources. X.W. and L.W.: manuscript revisions and grant application. All authors reviewed and consented to the publication of this manuscript version.

Funding: This study got financial support from the National Natural Science Foundation of China (8206120268).

Institutional Review Board Statement: All of our experiments performed in this study received approval from the Animal Experimentation Ethics Committee of Baotou Medical College, following the Guide for the Care and Use of Laboratory Animals (QDU-AEC-2022060).

Informed Consent Statement: Not applicable.

Data Availability Statement: All Data are available from the corresponding author upon a reasonable request.

Conflicts of Interest: No conflicts of interest.

References

1. Negi V, Singh P, Singh L, et al. A Comprehensive Review on Molecular Mechanism Involved in Arsenic Trioxide Mediated Cerebral Neurodegenerative and Infectious Diseases[J]. *Infectious Disorders-Drug Targets (Formerly Current Drug Targets-Infectious Disorders)*, 2024, 24(3): 51-59.
2. Mochizuki H. Arsenic neurotoxicity in humans[J]. *International journal of molecular sciences*, 2019, 20(14): 3418.
3. Najafi N, Barangi S, Moosavi Z, et al. Melatonin Attenuates Arsenic-Induced Neurotoxicity in Rats Through the Regulation of miR-34a/miR-144 in Sirt1/Nrf2 Pathway[J]. *Biological Trace Element Research*, 2023: 1-17.
4. Rezaee D, Saadatpour F, Akbari N, et al. The role of microRNAs in the pathophysiology of human central nervous system: a focus on neurodegenerative diseases[J]. *Ageing Research Reviews*, 2023: 102090.
5. Li S, Lei Z, Sun T. The role of microRNAs in neurodegenerative diseases: A review[J]. *Cell Biology and Toxicology*, 2023, 39(1): 53-83.
6. Lu J, Zhou N, Yang P, et al. MicroRNA-27a-3p downregulation inhibits inflammatory response and hippocampal neuronal cell apoptosis by upregulating mitogen-activated protein kinase 4 (MAP2K4) expression in epilepsy: in vivo and in vitro studies[J]. *Medical Science Monitor: International Medical Journal of Experimental and Clinical Research*, 2019, 25: 8499.
7. Ma M, Yin Z, Zhong H, et al. Analysis of the expression, function, and evolution of miR-27 isoforms and their responses in metabolic processes[J]. *Genomics*, 2019, 111(6): 1249-1257.
8. Chen L, Li Z, Hu S, et al. Extracellular vesicles carry miR-27a-3p to promote drug resistance of glioblastoma to temozolomide by targeting BTG2[J]. *Cancer Chemotherapy and Pharmacology*, 2022, 89(2): 217-229.
9. Luo J, Li J, *ong L, et al. MicroRNA-27a-3p relieves inflammation and neurologic impairment after cerebral ischaemia reperfusion via inhibiting lipopolysaccharide induced TNF factor and the TLR4/NF-κB pathway[J]. *European Journal of Neuroscience*, 2022, 56(3): 4013-4030.
10. Zhang Z, He J, Wang B. Circular RNA circ_HECTD1 regulates cell injury after cerebral infarction by miR-27a-3p/FSTL1 axis[J]. *Cell Cycle*, 2021, 20(9): 914-926.
11. Li W, Zhu Q, Xu X, et al. MiR-27a-3p suppresses cerebral ischemia-reperfusion injury by targeting FOXO1[J]. *Aging (albania ny)*, 2021, 13(8): 11727.
12. Lv X, Yan J, Jiang J, et al. MicroRNA-27a-3p suppression of PPAR-γ contributes to cognitive impairments resulting from sevoflurane treatment[J]. *Journal of Neurochemistry*, 2017, 143(3): 306-319.
13. Tichanek F, Salomova M, Jedlicka J, et al. Hippocampal mitochondrial dysfunction and psychiatric-relevant behavioral deficits in spinocerebellar ataxia 1 mouse model[J]. *Scientific Reports*, 2020, 10(1): 5418.

14. Misrani A, Tabassum S, Zhang Z, et al. Urolithin A Prevents Sleep-deprivation-induced Neuroinflammation and Mitochondrial Dysfunction in Young and Aged Mice[J]. *Molecular Neurobiology*, 2023: 1-19.
15. Firdaus F, Zafeer M F, Anis E, et al. Evaluation of phyto-medicinal efficacy of thymoquinone against Arsenic induced mitochondrial dysfunction and cytotoxicity in SH-SY5Y cells[J]. *Phytomedicine*, 2019, 54: 224-230.
16. Pan T, Wu F, Li L, et al. The role m 6 A RNA methylation is CNS development and glioma pathogenesis[J]. *Molecular Brain*, 2021, 14: 1-9.
17. Wang Q S, **ao R J, Peng J, et al. Bone Marrow Mesenchymal Stem Cell-Derived Exosomal KLF4 Alleviated Ischemic Stroke Through Inhibiting N6-Methyladenosine Modification Level of Drp1 by Targeting lncRNA-ZFAS1[J]. *Molecular Neurobiology*, 2023, 60(7): 3945-3962.
18. Peng D, Li M, **nbin L, et al. The miR-27a-3p/FTO axis modifies hypoxia-induced malignant behaviors of glioma cells[J]. *Acta Biochimica et Biophysica Sinica*, 2023, 55: 103-116.
19. Frisbie S H, Mitchell E J. Arsenic in drinking water: An analysis of global drinking water regulations and recommendations for updates to protect public health[J]. *PLoS One*, 2022, 17(4): e0263505.
20. Chen Y, Liu X, Zhang Q, et al. Arsenic induced autophagy-dependent apoptosis in hippocampal neurons via AMPK/mTOR signaling pathway[J]. *Food and Chemical Toxicology*, 2023, 179: 113954.
21. Chen Y, Cao P, **ao Z, et al. M (6) a methyltransferase METTL3 relieves cognitive impairment of hyperuricemia mice via inactivating MyD88/NF- κ B pathway mediated NLRP3-ASC-Caspase1 inflammasome[J]. *International Immunopharmacology*, 2022, 113: 109375.
22. Ma Y M, Zhao L. Mechanism and Therapeutic Prospect of miRNAs in Neurodegenerative Diseases[J]. *Behavioural Neurology*, 2023, 2023.
23. Rezaee D, Saadatpour F, Akbari N, et al. The role of microRNAs in the pathophysiology of human central nervous system: a focus on neurodegenerative diseases[J]. *Ageing Research Reviews*, 2023: 102090.
24. Chi B, Deng L, Zhi Z, et al. Upregulation of miRNA-26a enhances the apoptosis of cerebral neurons by targeting EphA2 and inhibiting the MAPK pathway[J]. *Developmental Neuroscience*, 2022, 44(6): 615-628.
25. Wu F, Wang F, Yang Q, et al. Upregulation of miRNA-23a-3p rescues high glucose-induced cell apoptosis and proliferation inhibition in cardiomyocytes[J]. *In Vitro Cellular & Developmental Biology-Animal*, 2020, 56: 866-877.
26. An K, Xue M J, Zhong J Y, et al. Arsenic trioxide ameliorates experimental autoimmune encephalomyelitis in C57BL/6 mice by inducing CD4+ T cell apoptosis[J]. *Journal of Neuroinflammation*, 2020, 17: 1-14.
27. Tang S, Shen Y, Wei X, et al. Olaparib synergizes with arsenic trioxide by promoting apoptosis and ferroptosis in platinum-resistant ovarian cancer[J]. *Cell Death & Disease*, 2022, 13(9): 826.
28. Ren X, Zhou X. Circ_0000011 promotes cerebral ischemia/reperfusion injury via miR-27a-3p-dependent regulation of NRIP1[J]. *Metabolic Brain Disease*, 2023, 38(1): 295-306.
29. Zhang H, Zhang M, Meng L, et al. Investigation of key miRNAs and their target genes involved in cell apoptosis during intervertebral disc degeneration development using bioinformatics methods[J]. *Journal of Neurosurgical Sciences*, 2020, 66(2): 125-132.
30. Aas A, Isakson P, Bindesbøll C, et al. Nucleocytoplasmic shuttling of FTO does not affect starvation-induced autophagy[J]. *PLoS One*, 2017, 12(3): e0168182.
31. Tian M Q, Li J, Shu X M, et al. The increase of Nrf2 m6A modification induced by FTO downregulation promotes hippocampal neuron injury and aggravates the progression of epilepsy in a rat model[J]. *Synapse*, 2023: e22270.
32. Ding H, Li Z, Li X, et al. FTO alleviates CdCl₂-induced apoptosis and oxidative stress via the AKT/Nrf2 pathway in bovine granulosa cells[J]. *International Journal of Molecular Sciences*, 2022, 23(9): 4948.
33. Selberg S, Yu L Y, Bondarenko O, et al. Small-molecule inhibitors of the RNA M6A demethylases FTO potently support the survival of dopamine neurons[J]. *International Journal of Molecular Sciences*, 2021, 22(9): 4537.
34. Jenner A, Peña-Blanco A, Salvador-Gallego R, et al. DRP1 interacts directly with BAX to induce its activation and apoptosis[J]. *The EMBO journal*, 2022, 41(8): e108587.
35. Ansari M Y, Novak K, Haqqi T M. ERK1/2-mediated activation of DRP1 regulates mitochondrial dynamics and apoptosis in chondrocytes[J]. *Osteoarthritis and Cartilage*, 2022, 30(2): 315-328.

36. Lim J, Bang Y, Kim K M, et al. Differentiated HT22 cells as a novel model for in vitro screening of serotonin reuptake inhibitors[J]. *Frontiers in Pharmacology*, 2023, 13: 1062650.
37. Li Z, **ao G, Wang H, et al. A preparation of Ginkgo biloba L. leaves extract inhibits the apoptosis of hippocampal neurons in post-stroke mice via regulating the expression of Bax/Bcl-2 and Caspase-3[J]. *Journal of Ethnopharmacology*, 2021, 280: 114481.

Disclaimer/Publisher's Note: The statements, opinions and data contained in all publications are solely those of the individual author(s) and contributor(s) and not of MDPI and/or the editor(s). MDPI and/or the editor(s) disclaim responsibility for any injury to people or property resulting from any ideas, methods, instructions or products referred to in the content.